A New Light Readout System for the LXeGRIT Time Projection Chamber

E. Aprile, A. Curioni, K.-L. Giboni, M. Kobayashi, K. Ni, and U. G. Oberlack

***Abstract*—LXeGRIT is a liquid xenon time projection chamber (LXeTPC) used as balloon-borne Compton telescope for imaging cosmic sources in the MeV energy band. The three-dimensional position sensitive charge readout is triggered by the xenon scintillation light. In the original chamber design, the light is detected by four UV sensitive, 2″ PMT's (EMI 9813), coupled to the liquid xenon vessel by quartz windows. In order to improve the trigger efficiency and uniformity, a new light readout system has been studied. It consists of 12 UV sensitive, compact 2″ PMT's (Hamamatsu R6041Q), mounted in Teflon frames which cover the four sides of the LXeTPC active volume. These all-metal PMT's were especially developed to work at liquid xenon temperature and up to 3.5 atm overpressure. Light simulations promise an increase in light collection efficiency by more than a factor of ten for the new readout. We present simulations of the light collection efficiency and initial results from the successful operation of the new PMT fully immersed in liquid xenon.**

***Index Terms*—Compton telescope, gamma-rays, liquid xenon, scintillation, time projection chamber (TPC), trigger.**

I. Introduction

LXeGRIT is a prototype of an advanced Compton telescope in which MeV gamma-rays are imaged in one homogeneous detector to maximize efficiency. These novel instruments measure three-dimensional locations and energy deposits of all gamma-ray interactions above threshold in the sensitive volume, to the extent that they can be spatially resolved. LXeGRIT realizes this concept with a combination of charge and light readout in a liquid xenon time projection chamber (LXeTPC) with sensitive volume of nearly $20 \times 20 \times 7$ cm^3. The xenon is liquified in a temperature around 178 K at our operating pressure between 1.7 and 2.3 bar, and provides an excellent medium for ionization and scintillation. The fast scintillation light, which peaks in the ultraviolet at 175 nm [1], provides the event trigger. Free ionization electrons are drifted in a uniform electric field of 1 kV/cm at the known drift velocity of about 2 mm/μs toward a shielding mesh (Frisch grid), which separates the drift volume from the sensing electrodes below. With a proper choice of electric fields, the charges are successively focused through the mesh and two orthogonal arrays of wires without loss. As they pass the wire structure, the drifting charges induce signals on neighboring wires, providing X- and Y-localization. Eventually, the charges are collected on a segmented anode, which accurately measures the energy deposits. The Z-position of each interaction is inferred from the drift time of the electrons with respect to the light trigger. For details on the detector principle and realization, we refer the reader to [2], [3].

The detector, originally developed as a laboratory prototype to test the feasibility of a large volume LXeTPC and to demonstrate its performance with gamma-rays, was later converted to a balloon payload for observations of cosmic gamma-ray sources. Over the course of several balloon flights in 1997, 1999, and 2000, LXeGRIT was successively upgraded in multiple aspects. (See [4], [5] for a description of the payload and its performance in the 2000 flight configuration.) The basic setup of the light readout, however, as an integral part of the detector itself, has remained unchanged, and has become a limiting factor in the performance of the current system.

II. Simulations of Light Collection Efficiency

The principal figure of merit for a light trigger system in our application is the PMT pulse height distribution for a given energy deposit anywhere in the sensitive volume. Since the trigger systems under consideration provide only limited spatial information, their ability to discriminate on energy is determined by the mean pulse height and its variance across the sensitive volume. Simulations allow us to study the spatial dependence of the pulse height, and optimize the system for high efficiency and uniformity. After equalization of PMT gains, the pulse height is given by the number of photoelectrons $N_{\rm pe}$ released on each PMT photocathode i

$$N_{{\rm pe},i}(\vec{r}) = \frac{E_\gamma}{W_{\rm eff}} \eta_{\rm qf} \eta_{\rm qe} P_{{\rm ce},i}(\vec{r}) \tag{1}$$

where $\langle N_{\rm ph} = (E_\gamma / W_{\rm eff})$ is the mean number of photons released by a gamma-ray interaction with energy deposit E_γ. We use $W_{\rm eff} = 23.7$ eV as the average energy required to generate a scintillation photon. $\eta_{\rm qf}$ is a field-dependent "quenching factor," which describes the reduction in scintillation yield due to electron extraction. We assumed $\eta_{\rm qf} = 0.4$. Finally, the photon is converted into a photoelectron with a "quantum efficiency" $\eta_{\rm qe}$. The photon collection efficiency $P_{{\rm ce},i}(\vec{r})$ for each PMT depends on the geometry of the setup, i.e., the solid angle of the PMT photocathode as seen from position $\vec{r}$, the distribution of reflective, transparent, and absorbent materials, the attenuation and scattering in the liquid itself, and the optical transparency of meshes and wire structures. This generally complicated function is determined by simulation. Once $N_{{\rm pe},i}(\vec{r})$ is computed,

Manuscript received December 13, 2002; revised July 13, 2003. This work was supported by NASA Grant NAG5-5108 to the Columbia Astrophysics Laboratory.

E. Aprile, A. Curioni,K.-L. Giboni, M. Kobayashi, and K. Ni are with the Columbia Astrophysics Laboratory, Columbia University, New York, NY 10027 USA (e-mail: age@astro.columbia.edu; curioni@astro.columbia.edu; kgiboni@astro.columbia.edu; masanori@astro.columbia.edu; nikx@astro.columbia.edu).

U. G. Oberlack is with the Department of Physics and Astronomy, Rice University, Houston, TX 77005 USA (e-mail: oberlack@rice.edu).

Digital Object Identifier 10.1109/TNS.2003.818235

0018-9499/03$17.00 © 2003 IEEE

the derivation of the spatial average is straightforward, and the trigger efficiency can be derived implementing the trigger logic and discriminator thresholds for the PMT signals.

For the simulation of the light collection efficiency, we initially followed two complementary approaches: a geometrical computation of ray traces, which allowed for fast computation with simple geometries, and a somewhat more computer-intensive Monte Carlo method, based on the propagation of photons through voxels of the detector. The two approaches served as a useful cross-check, producing simular results. In the following, we will focus on the Monte Carlo method. Each voxel of the detector is filled with a single medium described by a reflectivity, index of refraction, and attenuation length as applicable. For transparent and reflective media, also the local orientation of the media surfaces are required. The code further distinguishes between specular and diffuse reflectivity, with the simplification that materials were considered either specular-reflective or diffuse-reflective, but not both, and the specular reflectivity is implemented as a δ-function, i.e., with a single angle of reflection, rather than with a distribution about the mean value.

The refractive index for intrinsic scintillation light in liquid xenon has been measured with conflicting results: 1.566 ± 0.01 [6] and 1.69 ± 0.02 [7]. We assumed a value of 1.7, in agreement with the latter measurement. This is conservative, as the light collection efficiency would increase for a smaller refractive index due to reduced total reflection at the liquid xenonquartz interface: the critical incident angle at which total reflection occurs changes from 36° to 40°. The attenuation length in liquid xenon due to absorption is highly dependent on purity and values from a few centimeters to 3 m have been reported [8]. We tested attenuation lengths of 30 cm and 1 m, which result in light collection efficiencies that differ only by about 20% in the current setup but by a factor of about 3 for the new design. (This is due to the change in geometry and to the high reflectivity of the walls, which makes attenuation in the new design much more important.) The figures shown here refer to an attenuation length of 1 m.

Our current simulation does not take into account Rayleigh scattering, for which a scattering length of 30 cm in liquid xenon has been calculated theoretically [9]. The impact of Rayleigh scattering for our purpose of triggering is twofold: Photons that would reach a PMT in a straight line may be deflected and are lost in the current detector where reflectivity of the walls is minimal. The treatment as part of the attenuation length is, hence, appropriate. In the new design with enhanced reflectivity, some scattered photons may be recovered (if absorption is sufficiently small), thus increasing the light collection efficiency over our estimate. As a second (desired) effect, Rayleigh scattering should make the trigger efficiency somewhat more uniform, as photons from detector regions with small light collection efficiency may be deflected in direction of a PMT.

These simulations were first adapted to the current light readout system, since this allowed us to compare the simulation results with detailed, spatially resolved measurements of the light trigger efficiency as described in [10]. Such measurements were later repeated and extended for the settings of the year 2000 balloon flight. The study of the existing setup improved our understanding of its main weaknesses and, thus, provided additional insight to help with a new design.

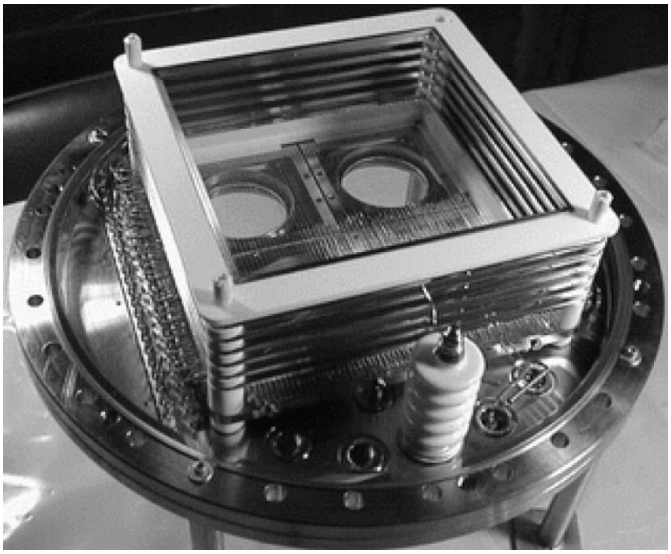

Fig. 1. The LXeTPC with the current light trigger system. Here the cathode was removed to show the readout structure and the windows through which the PMTs view the liquid xenon.

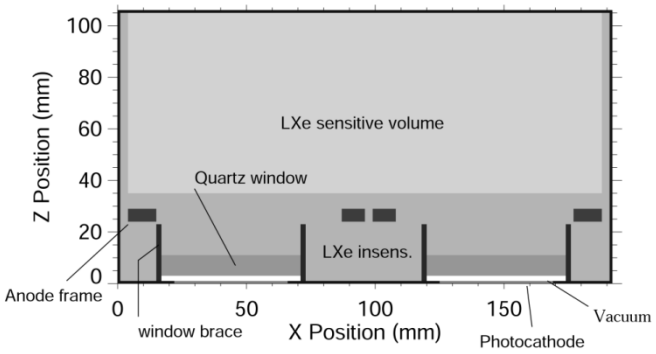

Fig. 2. Geometry of the old LXeTPC light trigger system as used in the Monte Carlo simulations of light collection efficiency, shown as a cross sectional view in the plane passing through the PMT centers. Event triggers from interactions in the insensitive layer of liquid xenon between the quartz windows and the anode meshes, held in place by the indicated anode frames, and from the charge collection region on top of the anode, indicated by the layer of "insensitive" liquid xenon, are referred to as "false" triggers. "Good" triggers are from interactions within the sensitive volume. The cathode is on top, here modeled as part of the totally absorbing walls.

A. The Current LXeGRIT Light Trigger System

In the current LXeGRIT light trigger system, the scintillation light is detected by four 2″ UV-sensitive PMTs (Electron Tubes 9813QA) with fused silica entrance windows and bialkali photocathodes, performing typically with 15% quantum efficiency at 175 nm. The PMTs view the xenon volume through four quartz windows, each 2.4″ in diameter and 8 mm thick, on the bottom of the chamber. Two of the windows, mounted on the detector flange, are visible in the photograph of Fig. 1. The window transparency for normal incidence is 88% and we assumed a refractive index of 1.5. The PMTs are mounted with a small gap below the windows, without direct optical coupling, due to concerns about mechanical stress on the windows when the balloon gondola hits the ground. Fig. 2 shows the geometry of the current detector as modeled in the simulation. Since the cathode and the field shaping rings around the drift region have

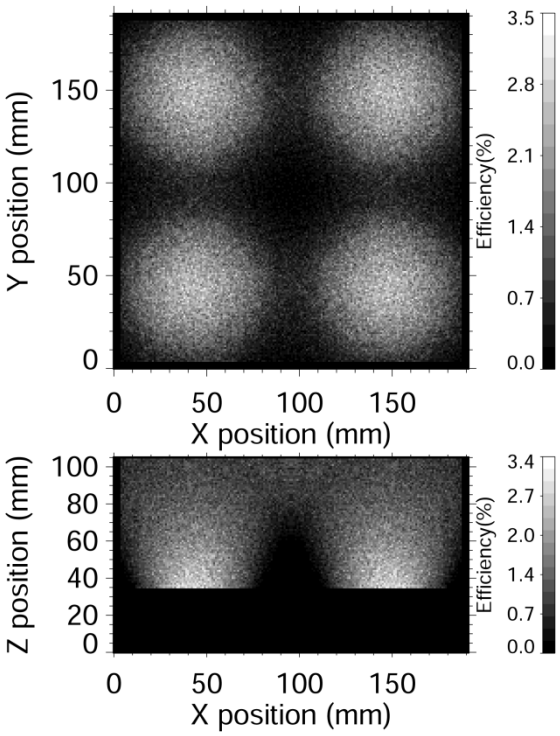

Fig. 3. Projections in X-Y, averaged over Z (top), and X-Z, averaged over Y (bottom), of the simulated light collection efficiency in the current setup. Here an attenuation length in liquid xenon of 1 m was assumed.

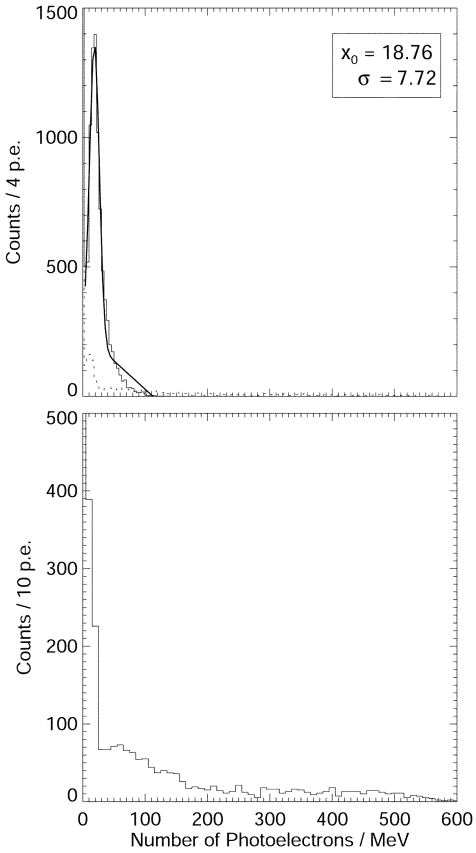

Fig. 4. Number of photoelectrons per MeV energy deposit seen on any of the four PMTs, for gamma-ray interactions in the sensitive volume (top) and within the passive xenon layer and charge collection region (bottom, and as a dotted line in the top panel). The chosen range of the ordinate cuts off the peaks at zero.

little reflectivity in the UV (we assumed zero reflectivity in the simulation), solid angle effects are expected to be significant and light collection efficiency low.

Fig. 3 shows projections of the computed light collection efficiency in X-Y and X-Z. Clearly, the light collection efficiency is highly nonuniform, and each PMT sees mainly the quarter of the chamber right on top. The sharp decline of trigger efficiency along a cone mantle, apparent in the bottom panel, is an effect of total internal reflection mainly at the quartz/air interface in front of the PMT. Total reflection occurs for incident light angles greater than $\arcsin(1/1.7) = 36°$. This effect alone reduces the mean light collection efficiency by about 40%, while increasing the relative spread by 50%. This cutoff in the simulation is sharper than observed, which may be due to the omission of Rayleigh scattering, and to a small reflectivity of the cathode on top and the stainless steel field shaping rings encompassing the sensitive volume. The top panel in Fig. 4 shows the resulting number of photoelectrons per MeV energy deposit. Despite the unfavorable geometry, there is still a distinct peak around 19 p.e./MeV and $\sigma \approx 8$ p.e./MeV, which contains 57% of all interactions in the sensitive volume.

A significant problem of the current setup is the number of background triggers due to gamma-ray interactions in the insensitive liquid xenon volume in the region between the PMTs and the anode meshes, as well as within the collection region between anodes and shielding grid. The former constitutes a 26 mm thick layer of liquid xenon at zero field, where the light yield is a factor of $\sim$2.5 higher than within the sensitive region. This gap is partially due to the metal braces which connect the quartz windows to the bottom flange of the chamber, and to the space required in order to connect the four anodes to a feedthrough in the center of the bottom flange. While the window mounting braces shield part of this xenon layer from the PMTs, a significant volume remains, which is located, with large photon collection efficiency and without charge quenching (no field), right in front of the PMTs. In the charge collection region above, between the anode meshes and the shielding grid, high field light quenching applies, but the solid angle is still favorable for much of this region, with exception of parts that are shaded off by total reflection at the quartz/air interface, the mounting braces, and the anode frames. The lower panel of Fig. 4 shows the pulse height distribution for these regions. While the overall volume is small compared to the sensitive volume, as the dotted line in the top panel shows, there are regions where the collection efficiency is greatly enhanced by factors up to $\sim$30 over the peak collection efficiency from the sensitive voume of $\sim$19 p.e./MeV. In this case, even X-rays of $<$50 keV will produce light signals comparable to 1 MeV gamma-rays in the sensitive volume. The fraction of background triggers depends on the spatial distribution of γ-ray interactions in the chamber and on the trigger settings, which determine the ratio of the trigger efficiency in the dead volume to the average over the sensitive volume. This is evident from Fig. 5, which shows the cumulative distribution functions for "good" and "false" triggers as a function of the pulse height for a uni-

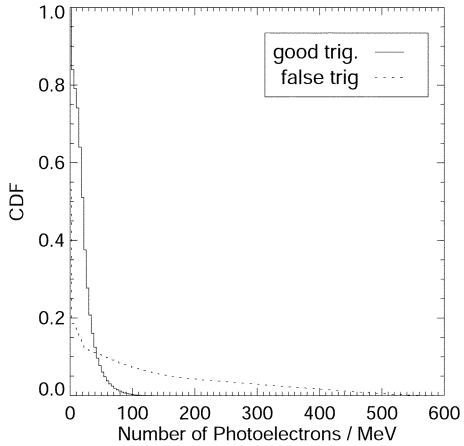

Fig. 5. Normalized number of triggers as a function of threshold level expressed in the number of photoelectrons per MeV, for gamma-ray interactions in the sensitive volume (solid line) and within the passive xenon layer and charge collection region (dotted line).

form distribution of gamma-ray interactions throughout the sensitive volume. This simulation indicates about 22% of background triggers for a range of low threshold settings, typical for the 1999 flight configuration, consistent with an earlier estimate [10]. For higher threshold settings, as in the 2000 flight, the fraction of background triggers increases, and was likely 30%–40% for a uniform distribution of gamma-rays. Work is in progress to estimate the true inflight fraction of background triggers with realistic γ-ray distributions, and from the flight data. While an online test for a minimum charge signal on the anodes keeps these background triggers from being recorded, it does affect adversely the speed of data acquisition.

B. The New Light Trigger System for LXeGRIT

Two main goals guided the design of a new light readout system: elimination of the background triggers and a great increase in the light collection efficiency. The development of a new compact PMT by Hamamatsu (R6041Q), for application in liquid xenon [11], [12], with a metal body that can withstand pressures of up to 3.5 atm enabled us to head for a design where the PMTs could be located much closer to the sensitive volume, fully immersed in liquid xenon. No windows are thus required, eliminating the problem of total internal reflection. Moreover, we aimed at making the chamber highly UV reflective, using teflon with a diffuse reflectivity of 90%. Placing the PMTs at the side, rather than at the bottom, makes the use of solid anodes with a certain UV reflectivity possible. Our currently best solution for the reflectivity of the electrodes is SiC, with a modest reflectivity of 40%. The compact design of the PMT, however, has had the draw-back of low quantum efficiency, of typically 8%, in the design that has been available so far, and which we used for our simulations and tests. A new version of the same PMT has recently been developed, and initial samples show quantum efficiency of 14.5% at 175 nm [13].

The optimized new design has three PMTs on each side, mounted in teflon blocks. A mechanical model is shown in the photograph of Fig. 6. In front of the PMT window, a highly transparent grounded mesh shields the PMT from the electric field of the chamber. The field shaping rings are replaced by thin

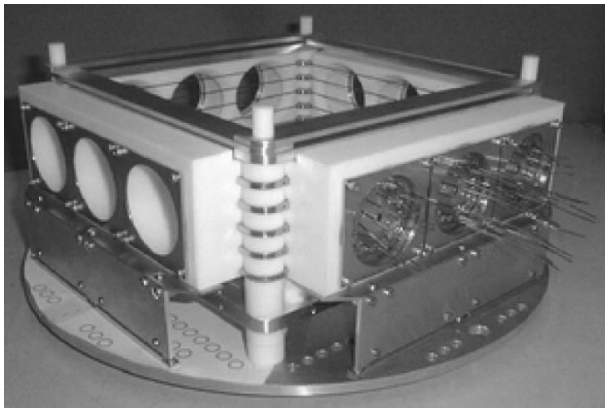

Fig. 6. A mechanical model of the new chamber design, with 3 PMTs at each side, embedded in teflon blocks.

wires, to maximize light transparency. Fig. 7 shows the X-Y projection of the light collection efficiency as modeled in the simulation. The distribution is much more uniform than in the old design. Each PMT views essentially the entire chamber, which also suggests a change in the way the light signals are read out. It is now favorable to first add all PMT signals in a summing amplifier, before setting a threshold on a discriminator. The resulting pulse height distribution for all PMTs combined is shown in Fig. 8. The peak of the distribution is now around 640 p.e./MeV for an attenuation length of 1 m, a factor of >30 higher than in the previous design. This allows for clear energy cuts and in fact energy measurements, and would also make pulse shape discrimination possible, if required. Nevertheless, the solid angle effects are still significant. This could possibly be reduced with a scheme that corrects for events that happen very close to one PMT. In this case, one PMT would have a much higher signal than the others, skewing the distribution in the summed signal. If the system can correct for this, by looking at both the summed and the individual signals, an even more accurate trigger response can be expected. We are also studying the possibility of improving the energy resolution of the detector by combining the energy information from charge and light. Work is in progress with a dedicated chamber to study the possible anti-correlation of light and charge signal and its effect on energy resolution, if combined. A recent measurement indicates that the anti-correlation exists, and that an improvement in energy resolution can indeed be achieved [14].

III. Tests of a PMT Immersed in Liquid Xenon

The new design of the LXeGRIT light trigger system depends crucially on the operation of the PMT inside the liquid xenon. Given the tight purity constraints for drifting electrons in liquid xenon (typically, the O_2 equivalent of impurities must be below 1 ppb), operating a PMT inside a LXeTPC is nontrivial. A successful measurement of γ-ray spectra with a PMT inside a liquid xenon chamber was reported by [15]. In this case, a conventional glass-envelope PMT was immersed with its head in liquid xenon, and else exposed to the xenon vapor on top. A metal-envelope PMT identical to ours has been successfully operated with much larger signals from α sources [12]. We are reporting here, to our knowledge, the first stable operation of a PMT fully immersed in liquid xenon, measuring the small signals of γ-rays.

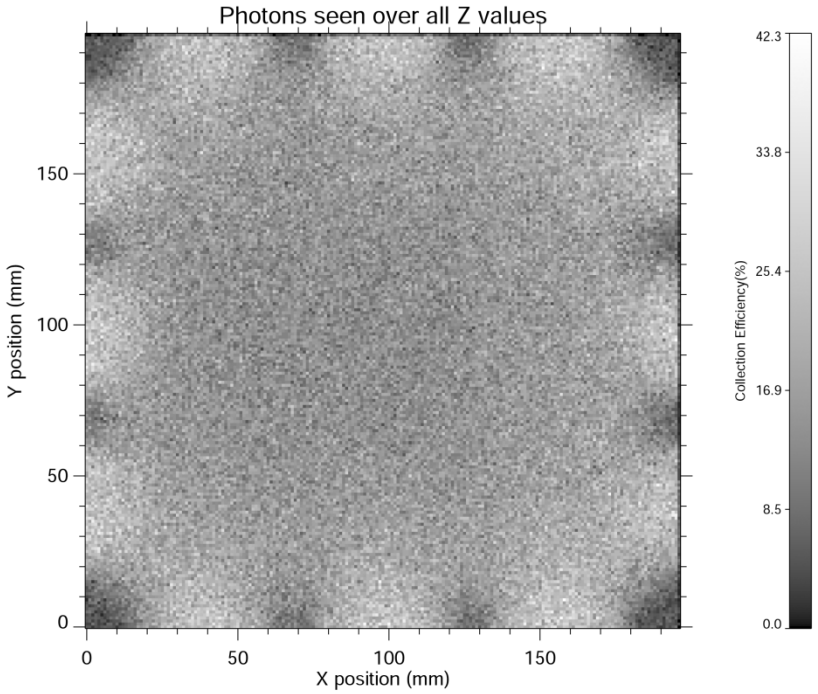

Fig. 7. X-Y projection of the simulated light collection efficiency for the new light readout system.

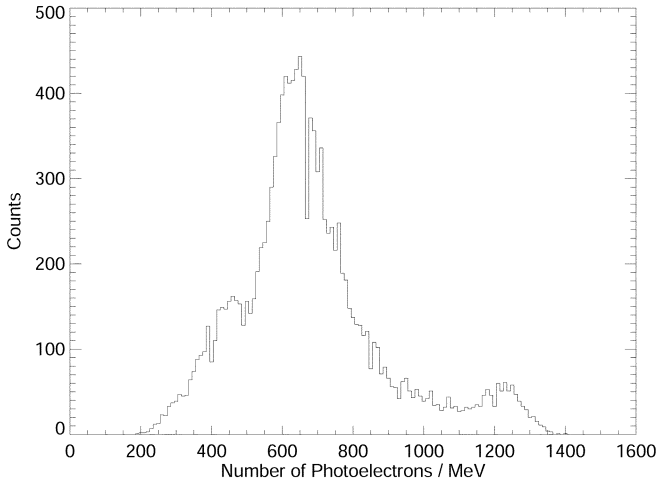

Fig. 8. Number of photoelectrons per MeV energy deposit, summed over the 12 PMTs for the new light readout system.

To test the R6041Q PMT in liquid xenon and study its impact on charge collection, we used an existing 3 L gridded ionization chamber [16], enclosed in a new vessel with the PMT mounted to view the 4.5 cm drift gap from one side. The charge response of the chamber was studied with external Cs, Na, and Co sources before introducing the new PMT, to have a reference for the charge yield. The first experiment carried out with the cleaned R6041Q inside the chamber, showed a significant loss of charge collection from the level achieved without the PMT (Fig. 9, top panel). Furthermore, the charge quickly decreased with time after filling the detector. This observation pointed to impurities introduced into the system which slowly dissolve in the liquid. These impurities made no measurable contribution to the outgas rate of the evacuated chamber, and also a Residual Gas Analyzer showed no significant deviations from the response measured with a clean chamber.

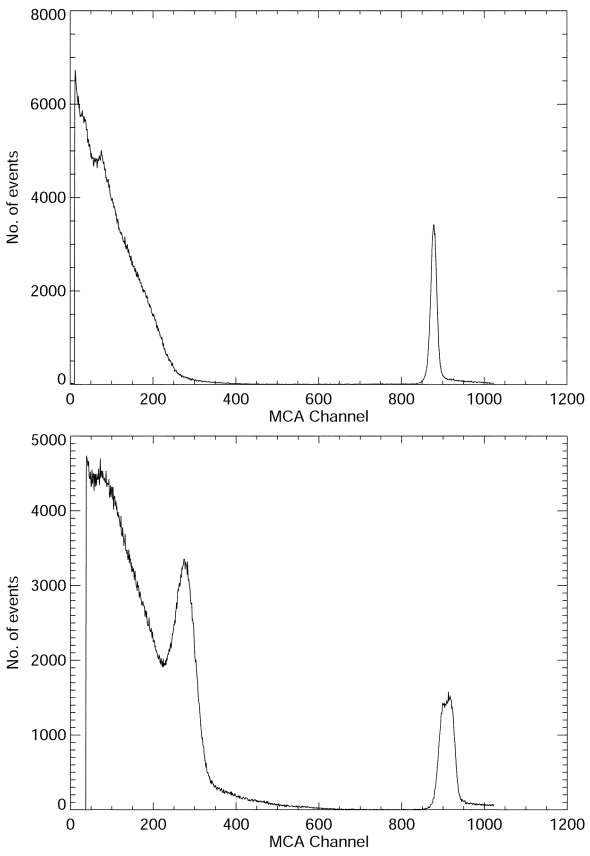

Fig. 9. ^{137}Cs charge spectra with PMT immersed in liquid xenon. Before (top) and after (bottom) various modifications and cleaning efforts to the PMTs, described in the text. Spectra were taken at various fields. The ones shown here were taken at 1 kV/cm. The peak to the right is from testpulses and indicates the contribution of electronic noise in this measurement.

In several tests with only parts of the components, the impurities could be traced back to the Teflon cables used as signal

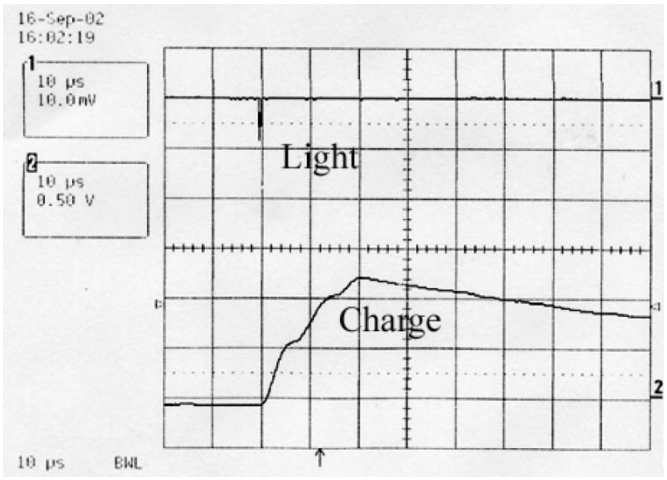

Fig. 10. Successful light triggering of gamma-ray events with PMT immersed in liquid xenon. Oscilloscope waveforms of a three-step gamma-ray event (bottom trace) with light trigger (top trace).

and HV connection for the PMT. A further contribution resulted from the printed circuit board carrying the voltage divider for the PMT. Finally, the apparent corrosion of the stainless steel surface of the PMT envelope was traced back to its exposure to HCl vapors during PMT assembly.

To remove all sources of impurities, the coaxial cables were replaced by simple copper wires insulated with ceramic beads, and the printed circuit board was replaced by a ceramic plate with the components attached by surface mount technology, similar to electronic hybrid circuits. Finally, the steel surface of the PMT was cleaned by very fine steel wool removing the corroded material. This process left the PMT envelope with the appearance of a clean steel surface. After these changes, the collected charge was restored to its original value (Fig. 9, bottom panel), and no decay with time was observed anymore. The light signals from the PMT now could be used to trigger on gamma rays, and their charge deposition could be observed in the detector volume (Fig. 10).

IV. Summary

Simulations of the current LXeGRIT light readout, together with earlier trigger efficiency measurements, clarified the shortcomings of the current setup. A new light readout design has been developed, using compact PMTs that can operate in liquid xenon. Simulations show that this revised design will provide a large improvement in light collection efficiency. We have achieved an important milestone toward this goal with the successful simultaneous readout of light and charge from γ-ray interactions with the PMT fully immersed in the liquid. This success is significant well beyond the improvement of the LXeGRIT trigger system, since liquid xenon is being actively studied as a detector material for Dark Matter search and other low background applications. The possibility of internal light readout without the need for viewports in the cryogenic vessel opens up completely new design options, and is pursued by our collaboration also as the main concept for the XENON Dark Matter Search detector [17].

The authors would like to thank R. Semple-Schuchter for the initial implementation of the Monte Carlo light simulation code.

References

[1] A. S. Schüssler, J. Burghoorn, P. Wyder, B. I. Lembrikov, and R. Baptist, "Observation of excimer luminescence from electron-excited liquid xenon," *Appl. Phys. Lett.*, vol. 77, no. 18, pp. 2786–2788, 2000.

[2] E. Aprile *et al.*. (1998) The electronics read out and data acquisition system for a liquid xenon time projection chamber as balloon-borne Compton telescope. *Nucl. Instrum. Methods A* [Online], pp. 425–436. Available: http://www.astro.columbia.edu/lxe/lxegrit

[3] E. Aprile, A. Curioni, K.-L. Giboni, U. Oberlack, and S. Ventura, "An upgraded data acquisition system for the balloon-borne liquid xenon gamma-ray imaging telescope LXeGRIT," *IEEE Trans. Nucl. Sci.*, vol. 48, pp. 1299–1305, Aug. 2001.

[4] E. Aprile *et al.*, "The LXeGRIT Compton telescope prototype: Current status and future prospects," in *X-Ray and Gamma-Ray Telescopes and Instruments for Astronomy*, J. E. Trümper and H. D. Tananbaum, Eds. Bellingham, WA: SPIE, 2003, vol. 4851, pp. 1196–1208. astro-ph/0 212 005.

[5] A. Curioni *et al.*, "On the background rate in the LXeGRIT instrument during the 2000 balloon flight," in *X-Ray and Gamma-Ray Telescopes and Instruments for Astronomy*, J. E. Trümper and H. D. Tananbaum, Eds. Bellingham, WA: SPIE, 2003, vol. 4851, pp. 1281–1293. astro-ph/0 211 584.

[6] L. M. Barkov, A. A. Grebenuk, N. M. Ryskulov, P. Y. Stepanov, and S. G. Zverev, "Measurement of the refractive index of liquid xenon for intrinsic scintillation light," *Nucl. Instrum. Methods A*, vol. 379, pp. 482–483, 1996.

[7] V. Chepel, V. N. Solovov, F. Neves, M. I. Lopes, R. F. Marques, and A. J. P. L. Policarpo. Liquid xenon scintillation: Light propagation and detection. presented at *IDM 2002: 4th Int. Workshop Identification of Dark Matter*. [Online]. Available: http://www.shef.ac.uk/phys/idm2002/talks/

[8] W. Ootani. $\mu \rightarrow e\gamma$ decay search with a liquid Xe scintillation detector. presented at *Symp. Japan Physics Society Meet. LXe Detectors and Their New Applications*. [Online]. Available: http://meg.web.psi.ch/docs

[9] G. M. Seidel, R. E. Lanou, and W. Yao, "Rayleigh scattering in rare-gas liquids," *Nucl. Instrum. Methods A*, vol. 489, pp. 189–194, 2002.

[10] U. Oberlack, E. Aprile, A. Curioni, and K. L. Giboni, "Performance of the light trigger system in the liquid xenon gamma-ray telescope LXeGRIT," *IEEE Trans. Nucl. Sci.*, vol. 48, pp. 1041–1047, Aug. 2001.

[11] T. Miyazawa *et al.*. (1998) Measurement of Gamma-Ray Sources with a Prototype Liquid Xe Calorimeter. Tech. Rep., Univ. Tokyo, Japan. [Online]. Available: http://meg.icepp.s.u-tokyo.ac.jp/docs/index.html

[12] K. Takizawa *et al.*, "Liquid Xe TPC with multistrip-type anode," in *X-Ray and Gamma-Ray Telescopes and Instruments for Astronomy*, J. E. Trümper and H. D. Tananbaum, Eds. Bellingham, WA: SPIE, 2002, vol. 4851. in press.

[13] S. Mihara, "Improved Quantum Efficiency for Hamamatsu PMT R6041Q," unpublished, 2002 private communication.

[14] E. Conti *et al.*, Correlated Fluctuations Between Luminescence and Ionization in Liquid Xenon, 2003. hep-ex/0 303 008.

[15] M. Lopes, V. Chepel, V. Solovov, R. F. Marques, and A. Policarpo, "A liquid xenon detector for positron emission tomography," in *Proc. 1999 IEEE 13th Int. Conf. Dielectric Liquids (ICDL'99)*, 1999, pp. 307–311.

[16] E. Aprile, A. Bolotnikov, D. Chen, R. Mukherjee, and F. Xu. (2002) Detection of gamma-rays with a 3.5 liter liquid xenon ionization chamber triggered by the primary scintillation light. *Nucl. Instrum. Methods A* [Online], pp. 636–650. Available: http://www.astro.columbia.edu/lxe/lxegrit

[17] E. Aprile *et al.*, "XENON: A 1 tonne liquid xenon experiment for a sensitive dark matter search," in *Proc. Int. Workshop Techniques and Applications of Xenon Detectors (Xenon01)*, 2002, p. 7670. astro-ph/0 207 670.